Developing a low cost 3D imaging solution for inscribed stone surface analysis

Adam P. Spring[*], Caradoc Peters

University of Plymouth, UK

ARTICLE INFO

ABSTRACT

The article uses a 3D imaging based solution where surface shading is determined by surface geometry. It is applied to inscribed stone surfaces in order to examine lettering and other carvings dated to the 5th - 9th centuries AD. Mid-range terrestrial laser scanning and structure from motion (SfM) based photogrammetry were cross-examined in order to create a low cost, but nevertheless highly accurate solution to 3D imaging that requires a computer, a camera, open source software like CloudCompare and a SfM based service called Photo located at ReCap360.autodesk.com. Ambient occlusion (AO) shading was used to show improvements made to the SfM data, which was achieved by adding known parameters to all photographs used. It simulates the direct light components of a light source so that exposed areas appear lightened and enclosed areas (like crevices and incisions) appear darkened. In the case study, AO was used to differentiate lettering in the inscription from damage and weathering on the granite surface of the Tristan Stone, as well as picking up a previously unnoticed wheel-head cross. This particular inscribed stone is located near Fowey in Cornwall, UK, and was known as the Long Stone before its name was changed on British Ordnance Survey (OS) Maps in 1951. The Tristan Stone was the first artefact to be scanned by the FARO Focus[3D] laser scanner after its release in 2010.

1. Introduction

Using the case study of the Tristan Stone, a 3D imaging solution is used that, unlike texture mapping, provides shading based on coordinates and actual surface information. In other words, a surface is actually mapped and then that data is used to show what is actually on that surface by controlling a light source based on surface features. It is not a relief or impression of 3D. The interpretation is actually based on surface geometry, or the digital mould created from the data. Unlike texture mapping techniques, such as RTI (MacDonald, 2011), or computer vision solutions like SfM (Davelli and Signoroni, 2013, 577), this technique does not involve a compromise in accuracy in order to get convenience or cheapness. Using what is referred to as a theoretical camera model by photogrammetrists, known parameters and known accuracies are increased along with repeatability of results.

Two sets of data were used as source material for the 3D imaging process. Mid-range terrestrial laser scanning (TLS) and structure from motion (SfM) based photogrammetry were applied to the Tristan Stone located in Cornwall, UK. The inscriptions on the stone have been associated with the tale of Tristan and Iseult from the Arthurian legends since the 20th century (Radford, 1975; Padel, 1981, 1991; Thomas, 1994), and are currently married to the 5th - 9th centuries based on stylistic dating methods (De Mandach, 1978; Padel, 1981, 1991; Okasha, 1993; Thomas, 1994). There are perhaps as many as 1500 inscribed stones like the Tristan Stone scattered across the landscapes of the Celtic-speaking regions of the British Isles (Forsyth, 2012). Fig. 1 shows that a problem with inscribed stones is migration, with their current position on the landscape not necessarily being their original location (De Mandach, 1978, p. 229; Davies et al., 2014). Current interpretations of their meaning are based primarily on historical documents and observation based techniques like raking light (Radford, 1975; De Mandach, 1978; Okasha, 1993; Padel, 1981; Thomas, 1994).

A low cost computer vision based solution was devised to identify remains on the surface of the granite artefact. It is outlined in this article and can be applied to other surfaces and materials. It was used to examine features on the stone, which are presented in Fig. 2. Inscriptions that are no longer visible when examining the monument in situ. Point cloud data generated from a FARO Focus[3D] phase shift laser scanner and from photographs taken with a Canon 60D digital single lens reflex (DSLR) camera are compared in order

* Corresponding author. Department of Archaeology, The Fal Building, College Road, Truro, TR1 3XX, UK.
E-mail address: adamspring@gmail.com (A.P. Spring).

to confirm the presence of new discoveries. A computer graphics technique called ambient occlusion (AO) shading, which can be used to enhance features based on surface depth (Langer and Bülthoff, 2000; Borgo et al., 2001), was applied to the 3D data by using software called CloudCompare. It was developed by Daniel Girardeau-Montaut when he was a PhD student working with Électricité de France (EDF), and has been open source since 2009 (Girardeau-Montaut, 2014). The methodology can be used to give an accurate understanding of what remains on the inscribed stone. Information is derived from solid surface meshes or moulds created from sensor data. This means that it is a technique not restricted to small objects or monuments. In fact, it can be applied to artefacts, structures or landscapes of all sizes (Zakšek et al., 2011).

2. Methods

2.1. Why the Tristan Stone is such a useful example for AO

Early Medieval in date, the Tristan Stone is one of many inscribed stones found all over the British Isles - predominantly South West England, Cornwall, Ireland, Scotland and Wales (Edwards, 2001, 2007). Used as memorial stones, the now weathered granite surfaces of the examples in Cornwall have often fallen prey to unresolvable disputes and speculations as to their meaning (Petts, 2002). The Tristan Stone is no exception.

The Tristan Stone was originally referred to as the Long Stone before its official change on Ordnance Survey Maps in 1951 (De Mandach, 1978, p. 227). The change reflected a linkage between the name of the individual commemorated on the stone with that of Tristan from the Arthurian legends. William Camden in 1586 was the first to record the name. He read it as 'Cirusius' (Gibson, 1722, p.18). Later in 1754, William Borlase made a more detailed drawing of the stone, again confirming the name as 'Cirusius' (Borlase, 1754, Fig. 2). It was only with a growing interest in ancient scripts, particularly uncials (influenced by Greek script), that new interpretations came in. In 1876, Hübner suggested that the first two letters were in fact an uncial 'D' with the curved side facing backwards (Hübner, 1876, p.7). This led to the idea that the name was actually 'Drustanus' and perhaps a Latinised form of 'Tristan'. Ralegh Radford (1951, p.117) and later Charles Thomas (Thomas, 1994; pp.279–280) championed this idea, even leading to the official OS name change for the stone. This interpretation was never fully accepted. Macalister (1945, pp.465–466) and Okasha (1993, pp.92–94) have both preferred to stick to the original interpretation on the basis that the script appears to be largely Roman capital letters and that they saw the 'C' and the 'I' as being distinctly separate.

Historians, however, have been unimpressed by the Tristan arguments. A study by Rachel Bromwich (1953) demonstrated that the Tristan legends were of diverse Celtic origins from different parts of the British Isles. Moreover, the idea that Tristan had been based in Cornwall only came about in the 12th century. Despite this key finding, archaeologists like Radford chose to ignore the historic evidence and debate the supposed physical evidence of the Tristan Stone inscription (Hutton, 2006, p.45). The Tristan Stone inscription remains the main archaeological evidence for the Tristan legend in Cornwall. This is why the 3D depth images generated by the laser scanner and by DSLR based photography are so important in providing an objective account of what remains on the surface.

Given the reinterpretation and renaming of the stone, the area perceived by some to depict the name 'Drustanus' was the point of interest when the scan data and photographs were used to document it. In Fig. 3a, AO shading was used to examine remains on the area where the archaic form of Tristan is meant to exist. This helped demonstrate clearly that the backwards curve and the vertical line

are separate. They represent a 'C' and an 'I', not a backwards uncial style 'D'.

Apart from discerning lettering in the inscription, AO helped pick out the full extent of the cross design on the back. A number of the past commentaries on the Tristan Stone have noted the presence of a tau-cross (a cross in the shape of the Greek letter 'τ') – for example William Borlase (1754, Fig. 4), Emil Hübner (1876, p.7) and Elizabeth Okasha (1993, p.92). One author, Samuel Lysons (1814, p.ccxxii) however notes 'a plain cross'. The AO from this study has revealed that the 'tau' shape was simply the unweathered portion of a wheel-head cross.

2.2. Camera model

It is important to distinguish between a fixed 'camera model' required for accurate measurement such as used here and a flexible 'camera model' used in vision techniques designed for navigation. The latter vision techniques ultimately need calibration to achieve any sort of accuracy.

'Camera model' is a term used to identify all variables associated with data collection in a 3D imaging workflow. The camera in this sense is seen as a measurement device collecting point or coordinate data. The model is also known as the collinearity model, and is used to work out the relationship between coordinates in the image or sensor plane (Schenk, 2006, p.59). This includes the relationship between the image and object points collected, which concur at the perspective centre of the sensor (Matthews and Noble, 2008, p.2). Fig. 4a and b show how the camera model can be used to discuss parameters for the interior orientation or properties of the sensors used. Table 1 is also used to explain image plane (sensor size) seen in Fig. 4a in more detail.

The relationship between the image and object points generated is also impacted upon by the exterior orientation or properties of the scene documented (Matthews and Noble, 2008; Spring et al., 2010). Exterior orientation includes variables like the distance between the sensor and the object, the distance between each camera position, light conditions, the reflective properties of a surface or any variables external to the sensor that affect the quality of the data collected (Matthews and Noble, 2008; Spring et al., 2010). The camera model can be used to refer to a laser scanner, which is also known as a depth camera (Cui et al., 2010), or indeed, to refer to a stills camera used in photography (Schenk, 2006, p.59). For example, the focal length of the lens, the size of the sensor and the amount of light let into the Canon 60D DSLR camera were known parameters when the Tristan Stone was documented.

The differences and similarities between laser scanning, photogrammetry and SfM are based on the camera model (Matthews and Noble, 2008; Spring et al., 2010; Westoby et al., 2012). As discussed in 3.1 for the FARO Focus[3D], the camera model for a laser scanner is based on the type of laser system used for data collection. Included in this is the beam diameter (3.8 mm), the method employed to collect data (phase shift) and the frequency the laser is set to (Dassot et al., 2011; Chow et al., 2012; Wunderlich et al., 2013). In this instance the Focus[3D] was set to 905 nm or infrared (IR) on the electromagnetic spectrum (Dassot et al., 2011). In laser scanning the camera model is a mechanically fixed parameter (Van Genechten et al., 2008) much like in affordable consumer driven photography. For example, the camera sensor used in a mobile phone.

Conversely, 3D point clouds generated from photographs and SfM can be improved by having a rudimentary knowledge of photography or photogrammetry (Matthews and Noble, 2008; Chandler and Fryer, 2013; Spring, 2014). This is especially the case in a DSLR based workflow where focal length is not fixed (Adam Technology, 2010). Where lenses are interchangeable,

(a)

Fig. 1. a. The Tristan Stone and its location in the British Isles, **b**. Its location in Cornwall, **c**. Migration pattern of the stone as outlined by De Mandach, 1978.

Fig. 1. (*continued*).

(c)

Tristan Stone - Locations

Site I
Sites II and IV
Site III
Site V
Present

Bing Maps Hybrid
(c) 2010 Microsoft Corporation

0 1 2 3 4 Kilometers

Fig. 1. (*continued*).

sensor size increases the amount of data that can be collected and users have greater control over the DSLR camera functions (Spring, 2014). In other words, higher resolution point clouds can be produced from photographs when the user has a greater understand of, and more control over, how the image is produced (see Fig. 4a

and Table 1). Known parameters and some form of calibration can be applied through the camera model in place (Matthews and Noble, 2008; Spring, 2014).

It is the camera model that differentiates a photo based 3D point cloud generated from SfM and a 3D point cloud intended to be used
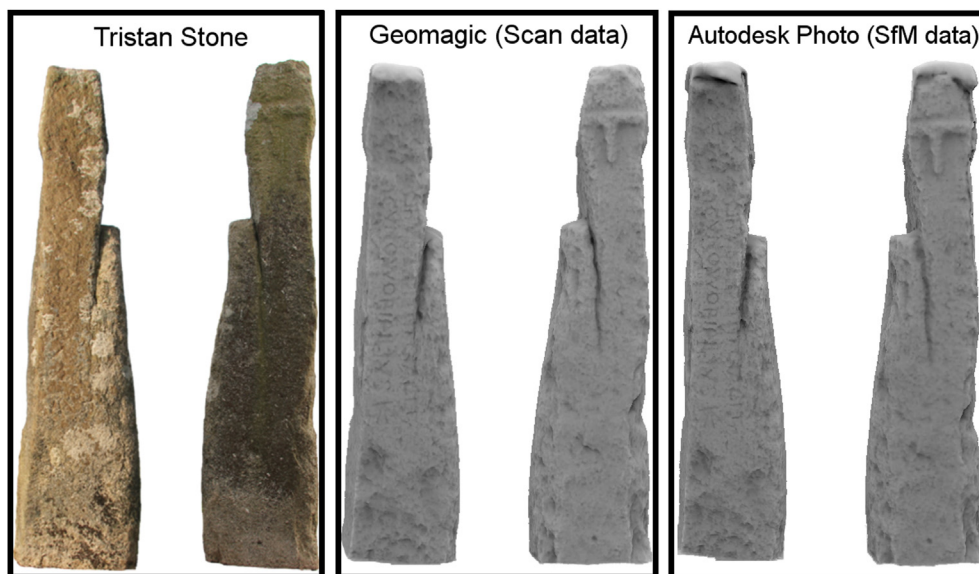
Fig. 2. A comparison of what the Tristan Stone looks like in situ, through scan data where AO has been applied and through SfM based data where AO has been applied.

for more accurate photogrammetric purposes (Hartley and Mundy, 1993; Chandler and Fryer, 2013). By combining elements from both workflows, the user benefits from the ease of use associated with SfM and the known resolution of data that is essential to photogrammetry (Hartley and Mundy, 1993). This is because photogrammetry is the art and science of using photographs to acquire metric information from a scene (Light and Jensen, 2005), which also predates digital computing (Hartley and Mundy, 1993; Luhmann et al., 2006). Whereas, SfM is a computer vision based technique originally designed for scene analysis and the remote navigation of unmanned systems and vehicles (Besl, 1987; Gage, 1995).

SfM has a flexible camera model until calibration parameters are added to the workflow being used (Chandler and Fryer, 2013; Crandall et al., 2013). As long as there is matching overlap in a group of photographs, a 3D point cloud can be generated using SfM even if a photograph is of low resolution (Snavely et al., 2006). SfM can generate a 3D point cloud based on images taken from multiple viewpoints, otherwise known as Multi View Stereo (MVS), and corresponding geometry of shapes within a scene (Snavely et al., 2006; Crandall et al., 2013; Koutsoudis et al., 2013). Overlap (ideally 60%), depth of field and base to distance ratio from the sensor to the object should always be considered when a photograph is taken (Matthews and Noble, 2008; Spring, 2014).

2.3. Digital documentation techniques

In the context of Cultural Heritage (CH), digital documentation techniques like mid-range TLS and SfM have a qualitative as well as quantitative value (Spring et al., 2010; Peters and Spring, 2014). The textured, 3D point clouds generated are open to interpretations that extend beyond the acquisition of metrically accurate data alone. For instance, the application of a FARO Focus[3D] to the Tristan Stone led to an examination of noise contained within the point cloud generated at the same time as the inscriptions on the granite surfaces. As seen in Figs. 2 and 3, AO shading also increased the resolution of the data and made text more visible to the human eye. Fundamental to the overall workflow was the capture and representation of surface texture, which had been greatly altered by processes like weathering over time. Knowing that the case study

was more a feature mapping exercise made the process of onsite data collection quicker as only local coordinate systems were required. At a minimum x, y, z, red, green and blue (RGB) and grayscale values can be obtained from point cloud data (Ullrich and Studnicka, 1999; pp. 49–56). It should be noted, however, that intensity of signal return is usually a value acquired as well (Höfle and Pfeifer, 2007). Integration and georeferencing of all datasets within
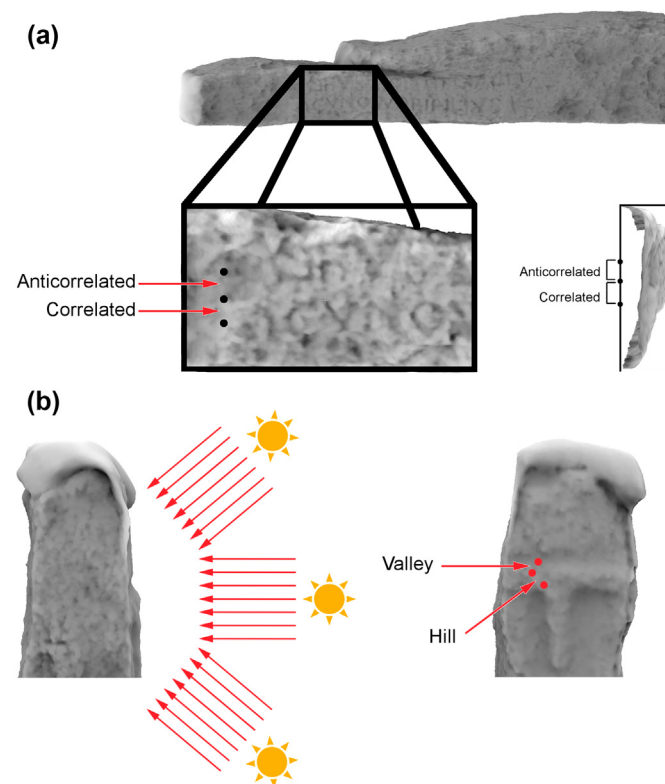

Fig. 3. a. The AO process explained in terms of anticorrelated and correlated points, **b**. AO process explained in terms of light fields and "Hill" and "Valley" points on surface.

absolute world coordinate systems can still be achieved if additional future proofing becomes a requirement later on.

Understanding how the FARO Focus[3D] collected data influenced what type of artefact it was applied to and the choice of case study (Spring et al., 2010). The excess number of points generated by the scanner - 976,000 per second - suggested high-resolution surface capture was possible (FARO Technologies, 2010). However, the relationship between the resolution of data captured and the surface feature analysed was ultimately determined by reducing data noise contained within the scan data (Chow et al., 2012; Wunderlich et al., 2013). Though the Tristan Stone represented the first instance in which the FARO Focus[3D] had been used for CH documentation since its commercial release (Spring and Peters, 2011), the success of the results was only made possible by the knowledge base and skill sets of the users. Noise reduction in the mesh generated was not an exercise that could be immediately conducted by non-specialists or users new to 3D imaging.

2.4. Scan resolution

The stone was scanned at a resolution of 6 mm point spacing over a distance of 10 m. At a capture phase, this meant any point generated closer than 10 m would be less than 6 mm to its nearest neighbour and any points beyond the 10 m mark farther apart. It was an easy and immediate way of setting the scanner to be compensated for what can be an overkill of information. Rapid acquisition of points is a primary advantage of using a laser scanner based methodology. It can, however, also make processing scan data a time consuming exercise. Keeping datasets at a more manageable and immediately processable size made information more accessible.

All point clouds were registered (connected together) in the FARO operating software Scene. It was then exported and meshed in a proprietary solution called Geomagic. Acquired by 3D Systems in 2013 (3D Systems, 2013), the software transforms point cloud data into solid surface meshes. It uses shape recognition algorithms that identify and focus on the main object in the point cloud (Geomagic, 2014) - in this case the Tristan Stone. This is done in order to filter extraneous noise from the data.

Prior to being laser scanned, a wheel-head cross on the back of the stone had been overlooked. This, in part, can be attributed to a) the course granite surface on which it is carved and b) oversight caused by the fact that the lower intact part can appear like a tau (or Greek letter 'τ') cross (cf. Okasha, 1993, p.92); the curve at the bottom of the tau being part of the wheel. The feature was enhanced in Geomagic using high resolution scan data.

3. Laser scanning

3.1. Interior orientation

The FARO Focus[3D] was launched in Austria, October 2010 (Spring and Peters, 2011). Scans of the Tristan Stone were conducted in December 2010 with one of the first systems available (Spring and Peters, 2011). The Focus[3D] used a phase shift solution that incorporated a class 3R (a safety qualification) laser 3.8 mm in diameter and set to 905 nm - a frequency in the IR band of the electromagnetic spectrum (Chow et al., 2012; Wunderlich et al., 2013; FARO Technologies, 2010). Measurements are acquired by comparing the outgoing and returning wave patterns of the laser as the scanner collects data (Van Genechten et al., 2008). The behaviour of, as well as noise contained within, the signal returned to the scanner was determined by the reflective property of the surfaces captured - 6 photons for an ideal return (Wallace et al., 2001). In the case of the Focus[3D], surfaces that were transparent, black or too reflective would cause issues like beam refraction, diffusion, weak or even too strong a signal return. When the latter occurs the receiver can become overexposed, which can cause additional noise at an information return phase (Chow et al., 2012; Wunderlich et al., 2013). The inclusion of matte white targets into
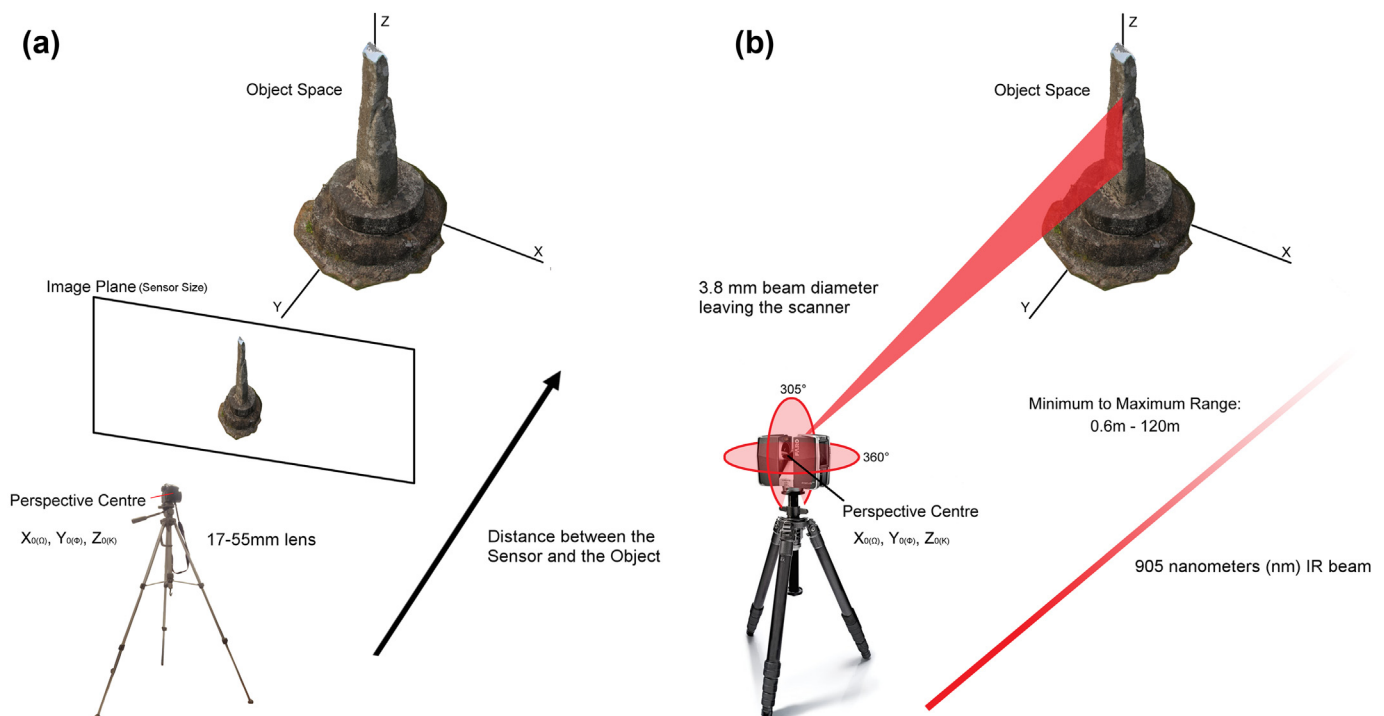

Fig. 4. a. Outline of 3D imaging camera model using a photography camera. **b**. Outline of 3D imaging camera model using a FARO Focus[3D] laser scanner .

Table 1

shows how pixel pitch, area and density are determined in the image plane (sensor size) presented in Fig. 4a. The focal length of the lens adds a dimension of scale and resolution that is tied to the image plane (sensor size). It is also linked to the relationship between the distance between the sensor and the object. This is especially the case when the focal length remains the same for all images generated. Switching from autofocus to manual focus once a scene is in focus is one simple way of calibrating a lens. Using a prime lens can also make it easier to improve this part of the data collection process. Auto rotate in the camera function should also be switched off.

Determining pixel values	Canon 60D
Pixel pitch $= \frac{\text{sensor width in mm}}{\text{sensor resolution width in pixels}} \times 100$	Canon 60D pixel pitch $= \frac{22.30}{5196} \times 1000 = 4.29\ \mu m$
Pixel area $= \frac{\text{sensor surface area in mm}^2}{\text{effective megapixels}}$	Canon 60D pixel area $= \frac{332.27\ \text{mm}^2}{18.00} = 18.4\ \mu m^2$
Pixel density $= \frac{(\text{sensor resolution width in pixels})^2}{\text{sensor width in cm}}/1000000$	Canon 60D pixel density $= (5196/2.23)^2/1000000 = 5.43\ MP/cm^2$

the workflow regulated these variables to an extent by including surfaces quantifiable to the way the scanner viewed the world (Van Genechten et al., 2008). This meant in terms of the IR frequency to which the Focus[3D] was calibrated.

3.2. Data noise

In the same way the pixels of a digital photograph taken in low light can appear grainy scan data contains noise that becomes visible under certain conditions (Chow et al., 2012; Wunderlich et al., 2013). Environmental conditions, focal length, aperture, ISO and the properties of the sensor determine the extent to which noise is presented in stills camera photography (Matthews and Noble, 2008; Spring, 2014). The equivalent in a mid-range TLS workflow is linked to the interior orientation of the scanner and external orientation parameters that affect data retrieval (Spring et al., 2010). Included in this is the number of points generated per second over a known distance.

The FARO Focus[3D] was used to document the Tristan Stone based on three known variables: the resolution of data captured, the size of the object documented and the distance at which information was collected. Similar to the hyperfocal length of a photography camera lens, mid-range TLS solutions have a distance at which optimum resolution can be achieved (Matthews and Noble, 2008; Chow et al., 2012; Wunderlich et al., 2013; Spring, 2014). This is a point where noise is not as apparent as it would be if the scene were captured from farther away (Chow et al., 2012; Wunderlich et al., 2013). The FARO Focus[3D] was no different and knowledge of this was considered prior to its application in a CH based workflow.

4. Structure from motion

4.1. Services and solutions

3D design companies like Autodesk have been making services and solutions more accessible to users since 2009 (Parks, 2012). The move to a symbiotic internet or web, where users work more closely with sensors to document an environment, instigated this change (Aghaei et al., 2012). It has led to user interfaces (UI) being redesigned and made easier to use - to save time at the data processing part of a workflow. 123D Catch - known as Photo Fly when it was released in 2011 (Autodesk Laboratories, 2011) - was the first SfM service to come out of Autodesk based on this development model (Autodesk, 2014a,b,c). Photographs processed through 123D Catch are reduced to 3 megapixel resolution (Chandler and Fryer, 2013). This restriction was removed in a professional version of the service, which was launched in beta with 5 gigabytes of free use in 2013 (Autodesk, 2014a,b,c). It is called Photo, and now offers a free trial or an annual subscription service priced at USD $55 (at time of publication). Photo is located at ReCap360.autodesk.com.

The free trial now allows for 50 photographs to be processed at a time. Whereas, the subscription service allows for 250 photographs at full resolution or "Ultra" setting (see Fig. 5).

4.2. Autodesk photo

Both 123D Catch and Photo are services that process data using distributed computing (Dikaiakos et al., 2009; Autodesk, 2014a,b,c). Also known as cloud computing, this means that photographs are loaded into the Photo UI located at ReCap360.autodesk.com, a 3D point cloud is generated through a network of computers that share the task of processing the data, and the results are then sent back to the user. The advantage of using Photo over comparable solutions like Agisoft Photoscan (see Agisoft Photoscan, 2014) is that it redirects the task of processing data away from the personal computer. High resolution 3D point clouds are generated in "the cloud", and the user is sent an email link to their data when it has been processed. In this context cloud computing can be used by heritage practitioners to save time and money. It also requires little to no understanding of the technical processes that go into 3D image production in terms of processing photographs.

Photo sends 3D data back to the user as a point cloud and solid surface mesh in .OBJ, .RCM, .FBX, .IPM or .RCS file format. Fig. 5 shows the selection screen presented to the user. There are also options to remove the unwanted data that is not the main focus of the scene, determine and adjust the focal length of the lens used and to add scale to the 3D data generated (Autodesk, 2014a,b,c). The latter is achieved via an easy to use point and pick window. A scale bar can also be used if it is added to the scene before photographs are taken. The UI allows the user to zoom in on a scale area, pick a point, pick another corresponding point elsewhere in the photograph and then add a value by typing it in. All 3D points generated after this step are scaled to this value.

4.3. Project Memento

In the FARO Focus[3D] workflow, a meshing package called Geomagic was used to remove unwanted data called noise from the 3D point cloud created by the laser scanner. While this process enhanced the surface features documented by the scan data, it also required the person processing the data to have specialist knowledge and skillsets in order to make the process work. Project Memento was launched in beta form by Autodesk Laboratories in 2013 (Autodesk Laboratories, 2014). It is designed to make it easier to incorporate solid surface data into a workflow - to make mesh analysis more accessible to artists and professionals working in sectors like heritage preservation. Once the 3D data had been produced via Photo, the solid surface mesh generated for the Tristan Stone was enhanced in Memento, much as the scan data had been in Geomagic. Fig. 6 shows that specific anomalies in the data, known as "spikes", were removed along with holes, particles

Fig. 5. The Autodesk Photo UI is designed to be easy to use and to provide data that can be used in multiple CAD and CAM based applications.

and tunnels. The UI for Memento was easy to use and similar to the UI created for Photo. Files could be imported in .OBJ and .RCM format and also exported in the 3D print format .STL. Table 2 presents the relationship between Autodesk solutions in more detail and outlines all services and solutions used.

5. Ambient occlusion (AO) shading

In computer graphics, AO shading is used to emulate the experience of depth created by environmental lighting conditions (Blinn and Newell, 1976; Debevec, 1998; Landis, 2002). It is a standard technique employed in the entertainment industry for computer animations, computer generated imagery (CGI) and for video game environment rendering (Landis, 2002). AO provides an added sense of depth to a scene by using light and dark shading to represent surface shape (Langer and Bülthoff, 2000). It is the digital equivalent to an artist using shading in order to convey the way light impacts upon a scene they are looking to reproduce (Langer and Bülthoff, 2000). AO shading, however, allows the user to
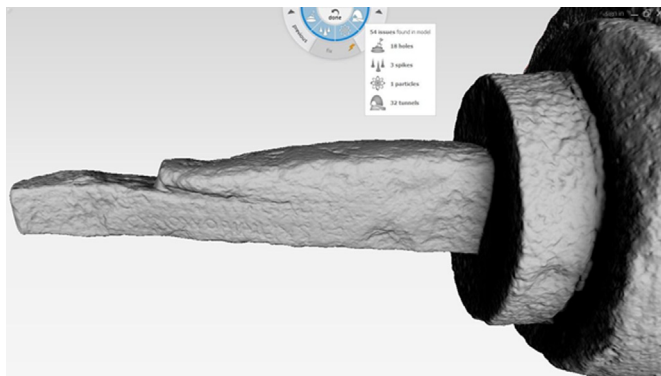

Fig. 6. Project Memento has an easy to use UI and automates mesh analysis and repair functions.

simulate and control light conditions as opposed to being restricted by a daily light cycle.

The technique was first used to enhance features on stone surfaces in 2004 (Duguet et al., 2004). It was applied to an Omphalos in the museum at Delphi, where it was used to enhance small features on the column based on variations of surface depth (Duguet et al., 2004). It works well on aged stone surfaces because only the direct light component of a scene is required. In addition to feature enhancement, it was used because it could also produce a natural lighting effect. This is the lighting effect mostly caused by diffuse reflection from irregular surfaces that would occur in the vicinity of the column. The variant used in CloudCompare is based on algorithms developed by Tarini et al., 2003. It does not require a lot of processing power and can be used on low end personal computers. It allows for quicker processing times because it directly accesses the Graphics Processing Unit (GPU) of the computer (Tarini et al., 2003).

The "Portion of Visible Sky" (qPCV) plugin in CloudCompare calculates the illumination of a point cloud or vertices in a mesh based on a theoretical hemisphere or sphere (Duguet et al., 2004; Girardeau-Montaut, 2014). Fig. 3a and b shows how this process works. The relationship between the points within the local coordinate system in place - statistically known as anticorrelated and correlated points - are used to generate 'light fields' from an infinite source with rays that behave in accordance with the geometry of the surface of the Tristan Stone data. CloudCompare enables the user to control the direction of light rays generated, which can be used to control resolution of detail. The more directions the light fields come from the better the resolution as that highlights the reflective exposed areas whilst emphasising areas of low reflectivity. The software also allows for light fields to be produced based on surface normal data collect from a point cloud, or to be sampled from a full sphere and northern hemisphere (Girardeau-Montaut, 2014). Fig. 3b demonstrates that an easy way to consider the behaviour of AO shading is to think of a surface in terms of having "Hills" and "Valleys" (Langer and Bülthoff, 2000). The way light fields behave within these area can be used to control the way they reflect off a surface - to the point where it can be simulated artificially.

Table 2
presents all services and solutions used for the workflows described in the article.

Services and solutions	Background information
CloudCompare	CloudCompare was initially developed between 2004 - 2007. It was supported by Électricité de France (EDF) who wanted it for internal uses as a monitoring and simulation tool. It made an immediate transition into heritage applications because of the EDF Foundation. It has been open source since 2009.
ReCap360.Autodesk.com	ReCap360 provides services and solutions geared toward what Autodesk is calling Reality Capture (ReCap). It is being used to refine point cloud data for computer aided design (CAD) and computer aided manufacture (CAM) applications. Laser scan is data is also supported at ReCap360.com
FARO Scene	FARO Scene is the operating and modelling software for FARO mid-range laser scanners. It is based on technology developed by a German company called iQvolution, which was acquired by FARO Technologies in 2005. It was used to register and export the native .FLS point cloud format prior to further modelling in Geomagic.
Geomagic	Geomagic came out of the North Carolina research triangle in 1997. It is a solution that transforms 3D point clouds into solid surface meshes for use in CAD and CAM based processes. Geomagic was acquired by 3D Systems in 2013, which is the same company that developed the .STL 3D printing file format.
123D Catch	123D Catch is a SfM based 3D imaging service that converts 2D photographs into point clouds and meshes. It is part of a wider suite of solutions brought together under the 123D brand, which are geared toward using 3D data for CAD and CAM based workflows. The professional equivalent of 123D Catch is Photo. Unlike 123D Catch, Photo does not reduce the resolution of photographs to 3 megapixels but does have an annual subscription fee.
Photo	Photo was introduced by Autodesk in 2013. It is geared toward infrastructure, asset management and high resolution data production. Included are otherwise grey area applications like cultural heritage and archaelogy. It is located at ReCap360.autodesk.com.
Project Momento	Project Memento was introduced by Autodesk Laboratories in 2013. It is designed to make mesh transformation easier and more accessible to anyone. Similar to 123D Catch and Photo, it is a more automated solution. It has an easy to use UI, which reduces data processing to a series of easy to use functions.

6. Discussion

With an increasing interest in user-friendly, low-cost solutions to 3D imaging, textures have been preferred rather than a high accuracy level for the surface geometry. It is not necessary to make such compromises. This article has gone some way to demonstrate this by outlining an easy to use workflow that anyone with access to a computer, an internet connection and photography camera can use. Given that the heritage sector is a price sensitive market, especially when it comes to equipment and application considerations, it should be noted that as 3D imaging becomes more affordable it has the potential to be accessed by a broader range of users as well. That is, if information and training are managed with accessibility to services and solutions in mind. Since the Tristan Stone was first documented with the FARO Focus^{3D} in 2010, automated services and solutions have developed to a point where useable results can be generated that are comparable to semi-automated equivalents like laser scanning. Solutions like Project Memento have also been designed with artists and heritage users in mind. The focus is now on the user experience (Kerr, 2002) and to create intuitive UI's that are not cumbersome to use.

6.1. Inscribed stone data

The inscribed stone data itself was used to explore 3D imaging techniques within the context of their application and intended deliverables. In this case, for demonstrating that the individual commemorated on the so-called 'Tristan Stone' was not Tristan, and confirming analyses of the historic evidence. It was also used to present the technologies discussed in a way where they can now be better understood - and used in accordance with this knowledge - by heritage practitioners. Similar results and feature resolution in both datasets suggest the age of affordable 3D will continue to lead to further revision and reinterpretation of material records and cultures. This is especially the case in examples that are well known for being greatly affected by subjective interpretations.

Acknowledgements

Appendix A. Supplementary data

Supplementary data related to this article can be found at http://dx.doi.org/10.1016/j.jas.2014.08.017.

References

3D Systems, 2013. 3D Systems to Acquire Geomagic. http://www.3dsystems.com/press-releases/3d-systems-acquire-geomagic (accessed 24.04.14.).

Adam Technology, 2010. How Accurate Is Photogrammetry? — Part 1. Adam Technology Team Blog. http://www.adamtech.com.au/Blog/?p=68 (accessed 28.05.14.).

Aghaei, S., Nematbakhsh, M.A., Farsani, H.K., 2012. Evolution of the world wide web: from web 1.0 to web 4.0. Int. J. Web Semantic Technol. 3 (1), 1–10.

Agisoft Photoscan, 2014. Product Comparison. http://www.agisoft.ru/products/photoscan (accessed 19.05.14.).

Autodesk, 2014a. 123D Catch. http://www.123dapp.com/catch (accessed 19.05.14.).

Autodesk, 2014b. Features for ReCap360. http://www.autodesk.com/products/recap/features/recap-360/all/list-view (accessed 19.05.14.).

Autodesk, 2014c. ReCap360. https://recap360.autodesk.com/ (accessed 19.05.14.).

Autodesk Laboratories, 2011. Project Photofly Graduates to Become 123D Catch Beta. https://web.archive.org/web/20111231061026/http://labs.blogs.com/its_alive_in_the_lab/2011/11/project-photofly-graduates-to-become-123d-catch.html (accessed 19.05.14.).

Autodesk Laboratories, 2014. Project Memento. https://beta.autodesk.com/callout/?callid=D69655022B4F42C880513D4E3085C7D (accessed 19.05.14.).

Besl, P.J., 1987. Range Imaging Sensors. General Motors Research Laboratories, Michigan.

Blinn, J.F., Newell, M.E., 1976. Texture and reflection in computer generated images. Commun. ACM 19 (10), 542–547.

Borgo, R., Cignoni, P., Scopigno, R., 2001. An easy to use visualization system for huge cultural heritage meshes. In: VAST'01 Proceedings of the 2001 Conference on Virtual Reality, Archeology, and Cultural Heritage, pp. 121–130. http://vcg.isti.cnr.it/publications/papers/statue_vast01.pdf (accessed 19.05.14.).

Borlase, W., 1754. Observations on the Antiquities Historical and Monumental of the County of Cornwall. W. Jackson, Oxford.

Bromwich, R., 1953. Some Remarks on the Celtic Sources of "Tristan". In: Transactions of the Honourable Society of Cymmrodorian (1953), pp. 32–60.

Chandler, J., Fryer, J., 2013. Autodesk 123D catch: how accurate is it? Geomatics World 2 (21), 28–30.

Chow, J., Lichti, D., Teskey, W., 2012. Accuracy assessment of the FARO Focus[3D] and Leica HDS6100 panoramic type terrestrial laser scanner through point-based and plane-based user self-calibration. In: FIG Working Week 2012: Knowing to Manage the Territory, Protect the Environment, Evaluate the Cultural Heritage. https://www.fig.net/pub/fig2012/papers/ts08c/TS08C_chow_lichti_et_al_5865.pdf (accessed 12.04.14.).

Crandall, D., Owens, A., Snavely, N., Huttenlocher, D., 2013. Discrete-continuous optimization for large-scale structure from motion. IEEE Trans. Pattern Anal. Mach. Intell. (PAMI). http://www.cs.indiana.edu/~djcran/papers/disco13pami.pdf (accessed 14.04.15.).

Cui, Y., Schuon, S., Chan, D., Thrun, S., Theobalt, C., 2010. 3D shape scanning with a time-of-flight camera. In: IEEE Computer Society Conference on Computer Vision and Pattern Recognition (CVPR) 2010. http://citeseerx.ist.psu.edu/viewdoc/download?doi=10.1.1.177.9506&rep=rep1&type=pdf (accessed 01.04.14.).

Dassot, M., Constant, T., Fournier, M., 2011. The use of terrestrial LiDAR technology in forest science: application fields, benefits and challenges. Ann. For. Sci. 68 (5), 959–974.

Davelli, D., Signoroni, A., 2013. Automatic mapping of uncalibrated pictures on dense 3D point clouds. In: 8th International Symposium on Image and Signal Processing and Analysis (ISPA), Trieste, Italy, pp. 576–581.

Davies, W., Campbell, J.G., Lockyear, K., Handley, M., 2014. Celtic Inscribed Stones Project. http://www.ucl.ac.uk/archaeology/cisp/database/stone/cstld_1.html (accessed 01.04.14.).

De Mandach, A., 1978. The shrinking tombstone of Tristan and Isolt. J. Mediev. Hist. 4 (3), 227–242.

Debevec, Paul, 1998. Rendering synthetic objects into real scenes: bridging traditional and image-based graphics with global illumination and high dynamic range photography. Proc. SIGGRAPH 98, 189–198.

Dikaiakos, M.D., Katsaros, D., Mehra, P., Pallis, G., Vakali, A., 2009. Cloud computing: distributed internet computing for IT and scientific research. IEEE Internet Comput. 13 (5), 10–13.

Duguet, F., Drettakis, G., Girardeau-Montaut, D., Martinez, J.L., Schmitt, F., 2004. A point-based approach for capture, display and illustration of very complex archaeological artefacts. In: Proceedings of the 5th International Conference on Virtual Reality, Archaeology and Intelligent Cultural Heritage, pp. 105–114.

Edwards, N., 2001. Early-medieval inscribed stones and stone sculpture in Wales: context and function. Mediev. Archaeol. 45 (1), 15–39.

Edwards, N., 2007. A Corpus of Early Medieval Inscribed Stones and Stone Sculpture in Wales: South-west Wales, vol. 2. University of Wales Press, Cardiff.

FARO Technologies, 2010. FARO Focus[3D]. Specification Sheet. http://www2.faro.com/site/resources/share/944 (accessed 19.05.14.).

Forsyth, K., 2012. Inscriptions, early medieval. In: Koch, J.T., Minard, A. (Eds.), The Celts: History, Life, and Culture. ABC-CLIO, LLC, Santa Barbara, CA, p. 450.

Gage, D.W., 1995. UGV history 101: a brief history of Unmanned Ground Vehicle (UGV) development efforts. Research Paper. Unmanned Syst. Mag. Retrieved from http://www.dtic.mil/dtic/tr/fulltext/u2/a422845.pdf (accessed 01.05.14.).

Geomagic, 2014. What Do the Three Types of Noise Reduction Mean in the Reduce Noise Command?. http://support1.geomagic.com/link/portal/5605/5668/Article/1014/What-do-the-three-types-of-noise-reduction-mean-in-the-Reduce-Noise-command (accessed 01.04.14.).

Gibson, E. (Ed.), 1722. W. Camden Britannia [1586]. Awnsham Churchill, London.

Girardeau-Montaut, D., 2014. CloudCompare. http://www.danielgm.net/cc/ (accessed 19.05.14.).

Hartley, R.I., Mundy, J.L., 1993. The Relationship Between Photogrammmetry and Computer Vision. International Society for Optics and Photonics. http://users.cecs.anu.edu.au/~hartley/Papers/SPIE-93/joint-paper/joint2.pdf (accessed 04.05.14.).

Höfle, B., Pfeifer, N., 2007. Correction of Laser Scanning Intensity Data: Data and Model-driven Approaches. http://www.ipf.tuwien.ac.at/publications/2007/Hoefle_Pfeifer_intensity_correction_Vol_62_6_2007.pdf (accessed 01.04.14.).

Hübner, E., 1876. Inscriptiones Britanniae Christianae. Williams & Norgate, London.

Hutton, R., 2006. Witches, Druids and King Arthur. Hambledon Continuum, London.

Kerr, A., 2002. Representing Users in the Design of Digital Games. http://www.digra.org/wp-content/uploads/digital-library/05164.06074.pdf (accessed 14.05.14.).

Koutsoudis, A., Vidmar, B., Ioannakis, G., Arnaoutoglou, F., Pavlidis, G., Chamzas, C., 2013. Multi-image 3D reconstruction data evaluation. J. Cult. Herit. 15 (1), 73–79.

Landis, Hayden, 2002. Production-ready Global Illumination. Course 16 notes. SIGGRAPH. http://renderman.pixar.com/view/production-ready-global-illumination (accessed 13.05.14.).

Langer, M.S., Bülthoff, H.H., 2000. Depth discrimination from shading under diffuse lighting. Perception 29 (6), 649–660.

Light, D.L., Jensen, J.R., 2005. Photogrammetric and remote sensing considerations. In: Bossler, J.D., Jensen, J.R., McMaster, R.B., Rizos, C. (Eds.), Manual of Geospatial Science and Technology. Taylor and Francis e-Library, London, p. 234.

Luhmann, T., Robson, S., Kyle, S., Harley, I., 2006. Close Range Photogrammetry: Principles, Techniques and Applications. Whittle Publishing, Scotland, pp. 15–24.

Lysons, S., 1814. Magna Britannia, vol. III. Cadell & Davies, Cornwall. London.

Macalister, R.A.S., 1945. Corpus Inscriptionum Insularum Celticarum, vol. I. Stationery Office, Dublin.

MacDonald, L.W., 2011. Visualising an Egyptian artefact in 3D: comparing RTI with laser scanning. In: EVA'11 Proceedings of the 2011 International Conference on Electronic Visualisation and the Arts, London, UK, pp. 155–162.

Matthews, N., Noble, T., 2008. Aerial and Close-range Photogrammetric Technology: Providing Resource Documentation, Interpretation and Preservation. Bureau of Land Management. Technical Note 428. http://www.blm.gov/nstc/library/pdf/TN428.pdf (accessed 25.04.15.).

Okasha, E., 1993. Corpus of Early Christian Inscribed Stones of South-west Britain. Leicester University Press, Leicester.

Padel, O.J., 1981. The Cornish background of the Tristan stories. Camb. Mediev. Celt. Stud. (1), 53–81.

Padel, O.J., 1991. Some south-western sites with Arthurian associations. In: Roberts, B.F., Bromwich, R., Jarman, A.O.H. (Eds.), The Arthur of the Welsh: the Arthurlan Legend in Medieval Welsh. University of Wales Press, Cardiff.

Parks, B., 2012. Creation Engine: Autodesk Wants to Help Anyone, Anywhere, Make Anything. http://www.wired.com/2012/09/ff-autodesk-and-the-big-make/all/ (accessed 18.05.14.).

Peters, C., Spring, A.P., 2014. Digital heritage, industrial memory and memorialisation. In: Orange, Hilary (Ed.), Reanimating Industrial Spaces: Conducting Memory Work in Post-industrial Societies. Left Coast Press. Ch. 11.

Petts, D., 2002. The reuse of prehistoric standing stones in western Britain? A critical consideration of an aspect of early medieval monument reuse. Oxf. J. Archaeol. 21 (2), 195–209.

Radford, C.A. Ralegh, 1951. Report on the excavations at Castle Dore. J. Royal Inst. Corn. 1, 1–119. New Series.

Radford, C.A. Ralegh, 1975. The Early Christian Inscriptions of Dumnonia. Cornwall Archaeological Society, Redruth.

Schenk, T., 2006. Introduction to Photogrammetry. Ohio State University. http://www.mat.uc.pt/~gil/downloads/IntroPhoto.pdf (accessed 14.04.14.).

Snavely, N., Seitz, S.M., Szeliski, R., 2006. Photo Tourism: Exploring Photo Collections in 3D. http://phototour.cs.washington.edu/Photo_Tourism.pdf (accessed 14.04.14.).

Spring, A.P., 2014. From Point clouds to manufactured products: an open-sourced solution. Computer 47 (9).

Spring, A.P., Peters, C., 2011. The Digitisation of Tristan and Iseult, Forensic Laser Scanning Engineering Surveying Showcase, September/October, pp. 34–35.

Spring, A.P., Peters, C., Minns, T., 2010. Using mid-range laser scanners to digitize cultural-heritage sites. IEEE Comput. Graph. Appl. 30 (3), 15–19.

Tarini, M., Cignoni, P., Scopigno, R., 2003. Visibility based methods and assessment for detail-recovery. In: Proceedings of the 14th IEEE Visualization, IEEE Computer Society. http://citeseerx.ist.psu.edu/viewdoc/download?doi=10.1.1.109.984&rep=rep1&type=pdf (accessed 19.05.14.).

Thomas, C., 1994. And Shall These Mute Stones Speak? Post-Roman Inscriptions in Western Britain. University of Wales Press, Cardiff.

Ullrich, A., Studnicka, N., 1999. 3D-Laser-Entfernungsbildaufnahme. In: Proceedings of Current Developments of Microelectronics, pp. 49–56. http://gme.tuwien.ac.at/hofg99/report.pdf (accessed 04.05.14.).

Van Genechten, B., Quintero, M.S., De Bruyne, M., Poelman, R., Hankar, M., Barnes, S., Caner, H., Budei, L., Heine, E., Reiner, H., García, J.L.L., Taronger, J.M.B., 2008. Theory and Practice on Terrestrial Laser Scanning: Training Material Based on Practical Applications. Universidad Politecnica de Valencia Editorial, Valencia, Spain.

Wallace, A.M., Buller, G.S., Walker, A.C., 2001. 3D imaging and ranging by time-correlated single photon counting. Comput. Control Eng. J. 12, 157–168.

Westoby, M.J., Brasington, J., Glasser, N.F., Hambrey, M.J., Reynolds, J.M., 2012. Structure-from-Motion photogrammetry: a low-cost, effective tool for geoscience applications. Geomorphology 179, 300–314.

Wunderlich, T., Wasmeier, P., Ohlmann-Lauber, J., Schäfer, T., Reidl, F., 2013. Objective Specifications of Terrestrial Laser Scanners – a Contribution of the Geodetic Laboratory at the Technische Universität München. Research Report. Metrica. Retrieved from http://www.metrica.gr/files/downloads/ObjectiveSpecsOfLS-EN.pdf (accessed 19.05.14.).

Zakšek, K., Oštir, K., Kokalj, Ž., 2011. Sky-view factor as a relief visualization technique. Remote Sens. 3 (2), 398–415.